# Robust Damping Controller for DFIG-Based Wind Turbine with Frequency Response

Lei Ba
*Electrical Engineering & Electronics*
*University of Liverpool*
Liverpool, United Kingdom
Lei.Ba@liverpool.ac.uk

Wei Yao
*Electrical and Electronics Engineering*
*Huazhong University of Science and Technology*
Wuhan, China
w.yao@hust.edu.cn

Lin Jiang
*Electrical Engineering & Electronics*
*University of Liverpool*
Liverpool, United Kingdom
ljiang@liverpool.ac.uk

***Abstract*—This paper proposes a robust damping controller for a doubly-fed induction generator (DFIG)-based wind turbine to mitigate system oscillation during frequency response (FR) and provide robust damping performance considering uncertain system operating points. Small signal stability results of DFIG with FR controller in a single machine infinity bus (SMIB) system and a 4-machine 11-bus (4M11B) system are obtained which indicate that a new lightly damped oscillation mode is excited by the FR controller, which will lead system oscillation and deteriorate system stability. In addition to the new excited oscillation mode, the system operating points are uncertain due to power grid strength variation, power system structure change and etc. Therefore, a robust damping controller is desired and proposed in this paper for DFIG equipped with FR controller. A conventional damping controller designed by residue method is also modelled in this paper. The effectiveness of the proposed robust damping controller is verified by comparing the small signal stability analysis results and simulation results to a conventional damping controller. Both small signal stability analysis results and simulation results indicate that the proposed robust damping controller shows the robust damping performance and less frequency deviation under different system operating points.**

***Index Terms*—DFIG, FR, robust controller, damping control.**

## I. Introduction

Wind power, as a rapidly developed renewable energy, has been widely integrated in power systems nowadays [1] [2]. Due to high penetration level of these wind power in power system, system FR capability is significantly affected as the variable speed wind turbines are connected to the power grid through power converters which makes them cannot contribute to frequency changes like traditional power plants. In order to improve system FR capability, system operators require the wind farms to participate in FR [3]. For instance, wind farms are give specific requirement for power reservation during grid frequency deviation in the UK and Ireland grid codes [4] [5].

Doubly-fed induction generator (DFIG), as the most common generator for variable speed wind turbine, has been widely deployed in wind power generation [6]. Unlike the synchronous generators, the rotor of DFIG is decoupled from grid through the back-to-back converter as shown in Fig. 1. When a large amount of power generated by DFIG is connected to grid, system effective inertia will be reduced as DFIG cannot contribute to FR. Due to the lack of FR capability, FR controllers are designed for DFIG-based wind turbine to support system frequency. The DFIG-based wind turbine equipped with FR controller is shown Fig. 1. When a frequency deviation occurred in the system, the FR controller will provide auxiliary power $P_{FR}$ to support system frequency.

Many researches have designed FR controller for DFIG-based wind turbine to support power system frequency [7] [8]. A hybrid modulated active damping control scheme for mitigating power oscillations caused by FR controller was proposed in [9]. To achieve better FR performance for DFIG based wind turbines, some studies are focusing on FR controller gain optimisation [10] [11] [12] [13] [14]. Throughout the literature reviews, most researches are focusing on FR gain optimisation for a better frequency support performance during DFIG participating in system FR. However, the impact of FR controller on system stability is not researched in most references. Although reference [9] and [14] proposed active power controllers adding at the rotor side converter (RSC) of DFIG to improve the power system low frequency oscillation caused by FR controller, these controllers are conventional damping controllers, which are limited to be designed at one system operating point. When the system operating point changes, a conventional damping controller will not be able to provide sufficient damping. Therefore, a robust damping controller is desired to be designed to provide robust damping performance under different system operating points.

In this paper, a robust damping controller is proposed and designed by $H_\infty$ control method using linear matrix inequalities (LMIs) with regional pole placements [15] [16], which can provide sufficient damping support during system oscillation and its damping performance is robust under different system operating points. As shown in Fig. 1, the proposed robust damping controller will provide additional damping power $P_{damping}$ added to the reference active power provided by $P_{MPPT}$ and $P_{FR}$. Comparing to the other robust controllers designed by using LQ and $H_2$ method, the $H_\infty$ control method can achieve its control performance by flexibly choosing its weighting functions in frequency domain.

This paper is organised as follows. Section II introduces the frequency response controller. Section III presents the proposed robust damping controller design. Section IV shows the small signal stability analysis results, simulation results

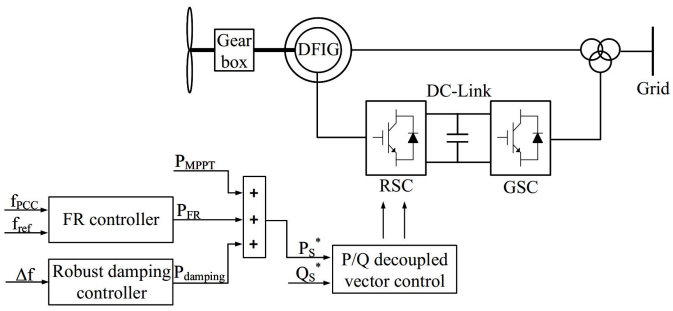


Fig. 1. DFIG-based wind turbine equipped with FR controller and robust damping controller

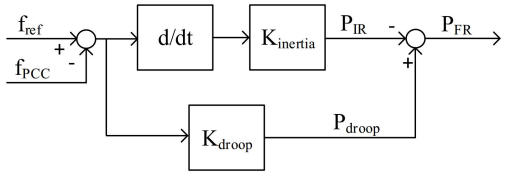


Fig. 2. Block diagram of FR controller

and discussion. Finally, a conclusion is made in Section V.

## II. Frequency response controller

According to reference [7]- [10], the block diagram of FR controller is shown in Fig. 2. Generally, a FR controller consists of two parts which are an inertia response (IR) and a droop controller. The details of IR controller, droop controller and small signal stability analysis of the DFIG equipped with FR controller are given in this section.

### A. IR controller

The IR controller is used to emulate the inertia response of a synchronous generator, which can limit the rate of frequency change when the power generated and load consumption is not balanced [7]. Thus, the power generated by IR controller should be negative. Equations (1) and (2) are used to express the working principle of an IR controller, which are obtained from swing equations of synchronous generators.

$$P_{IR} = K_{inertia} \times \frac{\mathrm{d}\omega_s}{\mathrm{d}t} \tag{1}$$

$$P_{IR} = K_{inertia} \times \frac{\mathrm{d}f_{PCC}}{\mathrm{d}t} \tag{2}$$

where $P_{IR}$ is the output power from IR controller, $\omega_s$ and $f_{PCC}$ are the synchronous generator speed and frequency at the point of common coupling (PCC) of wind turbine connection. $f_{PCC}$ is calculated using the phase angle measured by phase-lock-loop (PLL). $K_{inertia}$ is the IR controller gain. In this paper. the most appropriate IR controller gain proposed in [10] is used and calculated by equation (3), where H is the wind turbine inertia.

$$K_{inertia} = 1.85H \tag{3}$$

TABLE I
New excited oscillation modes of DFIG with FR controller

| Installed system | Oscillation frequency (Hz) | Damping ratio |
|---|---|---|
| SMIB | 1.0671 | 0.034 |
| 4M11B | 1.1987 | 0.048 |

### B. Droop controller

The droop controller can restore the frequency after the frequency deviation occurred [9] [10]. Hence, the power generated by the droop controller should be positive. $f_{ref}$ in Fig. 2 is the nominal system frequency which is set as 50 Hz in this paper. Equation (4) is used to express the working principle of a droop controller.

$$P_{droop} = \frac{f_{ref} - f_{PCC}}{R} = K_{droop} \times (f_{ref} - f_{PCC}) \tag{4}$$

In equation (4), $K_{droop}$ is the droop control gain and R is the wind turbine droop characteristic parameter. In order to optimise the droop control performance, a time-variant droop gain is used in this paper [11]. The linear time-variant droop gain can be calculated by using rotating speed as shown in equation (5).

$$K_{droop}(\omega_r) = A_{linear} \times \omega_r + B_{linear} \tag{5}$$

$A_{linear} = 28.5714$ and $B_{linear} = -17.1428$ are calculated by the method used in reference [11]. Finally, the sum of the power generated by both the IR and droop controller is used as auxiliary power and is added to the wind turbine MPPT power.

### C. Small signal stability analysis of the DFIG with FR controller

Through the small signal stability analysis of DFIG with FR controller installed in a SMIB system and a 4M11B system at different wind speeds, it can be found that the worst case is occurred when the wind turbine is operated at rated wind speed. For simplicity, the worst case small signal stability analysis results are provided here. Table I shows that a new oscillation mode is excited for the DFIG with FR controller installed in both systems. As seen in Table I, it can be seen that the new excited oscillation mode has low damping ratio. Analysing participation factors of the new excited mode, it can be found that state variables of FR controller dominate the new excited mode. Therefore, in order to mitigate system oscillation of DFIG with FR controller under different system operating points, a robust damping controller is need to be designed, which is introduced in the next section.

## III. Robust damping controller design

### A. Proposed robust damping controller

$H_\infty$ mixed-sensitivity control method is achieved by minimising the $H_\infty$ norm of a certain closed loop transfer function considering uncertainties using LMIs, where the $H_\infty$ norm can measure the worst-case of system gain [15]. $H_\infty$ mixed-sensitivity design formulation is expected to achieve output

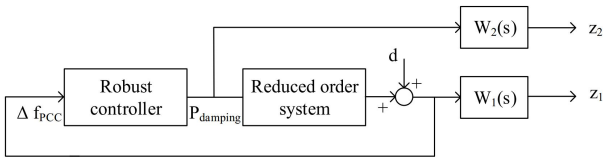


Fig. 3. Mixed-sensitivity damping controller configuration

disturbance and optimise control effort simultaneously [16]. It can be described as minimising the $H_\infty$ norm of sensitivity function S, which represents the transfer function between the disturbance input and measured output. In addition, the control effort optimisation can be achieved by minimising $\|KS\|_\infty$. Since the output disturbance is normally occurred at low frequencies and control action is required at high frequencies. Appropriate weighting functions can be selected to achieve two minimisation problems over the frequency range.

Fig. 3 shows the diagram for the mixed-sensitivity damping controller configuration. The input and output of robust controller are selected using observability, which is PCC frequency deviation and DFIG active power. d is the disturbance input. $z_1$ and $z_2$ are the outputs to be regulated, which represents the impact of disturbance on system output $\Delta f_{PCC}$ and control effort, respectively. Weighting functions $W_1(s)$ and $W_2(s)$ are selected as a low pass filter and a high pass filter, respectively. $W_1(s)$ is chosen for output disturbance rejection. $W_2(s)$ can be selected to reduce the control effort at high frequencies [16]. Equation (6) shows the weighting function chosen for designing the robust controller. In addition to achieving robustness, regional pole placement is also added to ensure a minimum 0.15 damping ratio using a conic sector.

$$W_1(s) = \frac{15}{s+15}, W_2(s) = \frac{8s}{s+80} \tag{6}$$

The full order of DFIG-based wind turbine equipped with FR controller is 17th order. Large calculation time will be required and complex controller will be designed if the plant order is high. In addition, only few states contain the interested system characteristics. Hence, the Schur method was used for model truncation [17]. According to the frequency responses of the full order and reduced order systems at different order, it can be found that the system order for more than 8th order can maintain the similar frequency response as the full order system in the interested frequency range. Hence, an 8th order reduced model is selected to design the controller. The transfer function of the 8th order reduced model is shown in the following equations.

$$H_{system}(s) = \frac{N(s)}{D(s)} \tag{7}$$

$$\begin{aligned} N(s) = &-8.5287 \times 10^{-5}s^8 - 0.0088s^7 - 0.0641s^6 \\ &- 3.5872s^5 - 6.4373s^4 - 1.268s^3 - 0.0122s^2 \\ &- 2.3071 \times 10^{-4}s + 6.0208 \times 10^{-8} \end{aligned} \tag{8}$$

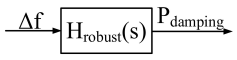


Fig. 4. Block diagram of Robust damping controller

$$\begin{aligned} D(s) = &s^8 + 3.8106s^7 + 437.6901s^6 + 1.0399 \times 10^3 s^5 \\ &+ 9.7706 \times 10^3 s^4 + 1.9363 \times 10^4 s^3 \\ &+ 4.3192 \times 10^3 s^2 + 53.2105s + 0.8958 \end{aligned} \tag{9}$$

Using the reduced order model and selected weighting functions, the linearised model considering the effect of weighting function can be obtained. Since the system order of the reduced order system model considering the weighting function became 10th-order, the current model can be further truncated to a 4th-order. The robust controller can be calculated using *hinfmix* function in MATLAB LMI Control Toolbox. The transfer function of the designed robust controller is given in equations (10)-(12). The block diagram of the proposed robust damping controller is shown in Fig. 4.

$$H_{robust}(s) = \frac{N_c(s)}{D_c(s)} \tag{10}$$

$$\begin{aligned} N_c(s) = &1.1449 \times 10^8 s^3 + 9.9789 \times 10^9 s^2 \\ &+ 4.4635 \times 10^9 s + 1.9263 \times 10^8 \end{aligned} \tag{11}$$

$$\begin{aligned} D_c(s) = &s^4 + 1.7811 \times 10^6 s^3 + 9.0086 \times 10^7 s^2 \\ &+ 4.7058 \times 10^6 s + 1.6973 \times 10^4 \end{aligned} \tag{12}$$

### *B. Conventional damping controller*

A conventional damping controller, which is designed by the residue method, is also provided in this paper to compare the robustness of proposed damping controller. The details of conventional damping controller design can be found in [18]. The feedback transfer function of the conventional damping controller can be expressed by equation (13).

$$H_{conventional}(s) = K\frac{T_w}{1+T_w s}\left(\frac{1+T_1 s}{1+T_2 s}\right)^2 \tag{13}$$

The compensation constants $T_1$ and $T_2$ are calculated as $T_1 = 0.1048s$ and $T_2 = 0.0811s$. The gain K is set as 10. The time constant $T_w$ is set as 10 s. Based on the design of a damping controller, the limitation is that it was designed based on the system linearisation results at one operating point. When the system operating point changes, such as the connected power grid changing from a strong grid to a weak power grid, the conventional damping controller will not be able to provide sufficient damping performance for the new system operating point. Therefore, a robust damping controller is desired for dealing with uncertain system operating points.

## IV. Performance evaluation

### *A. A SMIB system*

*1) Small signal stability analysis:* Table II and III show the new excited oscillation mode of DFIG connected to a strong and a weak power grid with a conventional and the proposed

TABLE II
NEW EXCITED OSCILLATION MODE OF DFIG CONNECTING TO A STRONG POWER GRID

| Controller type | Oscillation frequency (Hz) | Damping ratio |
|---|---|---|
| Conventional | 1.6828 | 0.1158 |
| Robust | 1.6649 | 0.1906 |

TABLE III
NEW EXCITED OSCILLATION MODE OF DFIG CONNECTING TO A WEAK POWER GRID

| Controller type | Oscillation frequency (Hz) | Damping ratio |
|---|---|---|
| Conventional | 1.0611 | 0.0476 |
| Robust | 1.0528 | 0.1719 |

robust damping controller. Comparing the small signal stability analysis results in Table I to Table II and III, it can be found that adding a damping controller can improve the damping ratio of the new oscillation mode for both a strong and weak grid connection.

Comparing the small signal stability analysis results in Table II to III, it can be found that the damping performance of the new excited oscillation mode with the proposed damping controller is robust against power grid strength change. However, a conventional damping controller cannot ensure sufficient damping performance for different power grid strength.

*2) Simulation results:* Fig. 5 shows the simulation results of system frequency response during power grid strength variation. The power grid strength is changed from a weak grid to a strong grid at 0.5 second and the grid strength is changed back to a weak grid at 15 seconds. According to the simulation results shown in Fig. 5, it can be found that the damping performance of the proposed damping controller is robust in regardless of the power grid strength change. The oscillation is mitigated within 5 seconds. However, the damping performance of a conventional damping controller for the case of changing the power grid strength from a strong grid to a weak grid at 15 seconds cannot meet the oscillation settling time requirement, where oscillations should be settled within 12-15s [16]. The oscillation takes more than 15 seconds to be mitigated, whereas the oscillation for the case of changing the power grid strength from a weak grid to a strong grid at 0.5 second can be mitigated within 10 seconds. The simulation results obtained is consistent to the small signal stability results shown in Table II and III.

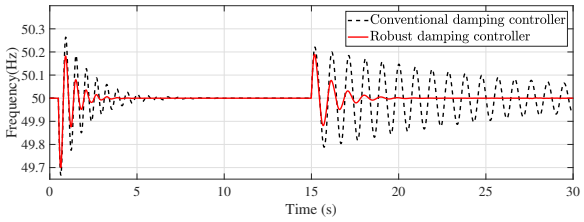


Fig. 5. System frequency response with grid strength change

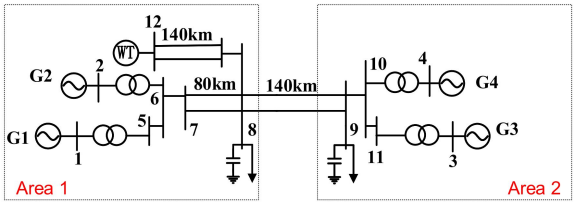


Fig. 6. A 4M11B system with DFIG-based wind power system

TABLE IV
NEW EXCITED OSCILLATION MODES OF THE 4M11B SYSTEM WITH A CONVENTIONAL DAMPING CONTROLLER FOR DIFFERENT TIE-LINE POWER

| Tie-line power | Oscillation frequency (Hz) | Damping ratio |
|---|---|---|
| 200MW | 1.2452 | 0.0691 |
| 300MW | 1.2226 | 0.0646 |
| 400MW | 1.1919 | 0.0584 |
| 500MW | 1.1433 | 0.0485 |

### *B. A 4M11B system*

Fig. 6 shows the single line diagram for integrating the DFIG-based wind farm in a 4M11B power system, the generators, loads and line impedance parameters are set as [19], which are provided in Appendix B. The synchronous generators G1-G4 are installed with PSS to damp the system inter-area oscillation mode. Comparing to the classic 4M11B system provided in [19], the DFIG-based wind farm is connected to the system at node 8 through a long transmission line, which will be supposed to connect wind farm to a weak grid, the short circuit ratio at point 12 is less than 3. The nominal operating point is selected as 400 MW tie-line power flow between two areas. The output power of wind farm equals to 504 MW for 15% wind power penetration level.

*1) Small signal stability analysis:* The small signal stability analysis results comparing the damping performance of a conventional and a robust damping controller in a 4M11B system with different tie-line power flows between two areas are given in Table IV-V. Comparing the results shown in Table IV-V, it can be found that the robust damping controller can always provide the sufficient damping performance when the tie-line power flows are changed. A minimum 0.15 damping ratio of the new excited mode can be maintained by using the proposed robust damping controller, whereas the damping ratio of new excited mode using conventional damping controller cannot meet the damping ratio requirement.

In addition, the small signal stability analysis results of new excited mode for high DFIG penetration levels are given in

TABLE V
NEW EXCITED OSCILLATION MODES OF THE 4M11B SYSTEM WITH A ROBUST DAMPING CONTROLLER FOR DIFFERENT TIE-LINE POWER

| Tie-line power | Oscillation frequency (Hz) | Damping ratio |
|---|---|---|
| 200MW | 1.2231 | 0.1659 |
| 300MW | 1.2004 | 0.1622 |
| 400MW | 1.17 | 0.1568 |
| 500MW | 1.123 | 0.1505 |

TABLE VI
NEW EXCITED OSCILLATION MODES OF THE 4M11B SYSTEM WITH A CONVENTIONAL DAMPING CONTROLLER

| DFIG penetration level | Oscillation frequency (Hz) | Damping ratio |
|---|---|---|
| 15% | 1.1919 | 0.0584 |
| 20% | 1.0507 | 0.0628 |
| 25% | 0.8909 | 0.0792 |
| 30% | 0.7205 | 0.1198 |

TABLE VII
NEW EXCITED OSCILLATION MODES OF THE 4M11B SYSTEM WITH A ROBUST DAMPING CONTROLLER

| DFIG penetration level | Oscillation frequency (Hz) | Damping ratio |
|---|---|---|
| 15% | 1.17 | 0.1569 |
| 20% | 1.0356 | 0.16 |
| 25% | 0.88 | 0.1721 |
| 30% | 0.7263 | 0.1763 |

Table VI and VII, where a high wind power penetration level means that more than 10% load consumption is provided by wind power [20]. Comparing the damping ratio of the new excited mode for using a conventional and a robust damping controller, it can be concluded that the damping performance of the proposed damping controller is robust for different wind power penetration levels. A minimum 0.15 damping ratio of new excited mode can also be ensured for different wind power penetration levels. However, the damping performance of the conventional damping controller is varied when the DFIG penetration level changed.

*2) Simulation results:* The simulation results for the DFIG installed in a 4M11B system are provided for investigating the robustness of the proposed damping controller. A three-phase short circuit fault at node 9 is added at 0.5s and cleared at 0.6s. Fig. 7 shows the simulation results of system frequency under nominal operating condition. According to the simulation results in Fig. 7, it can be found that the robust damping controller provides better damping performance and less frequency deviation than a conventional damping controller. Frequency oscillation can be mitigated within 6 seconds with the proposed robust damping controller, whereas the conventional damping controller takes more than 20 seconds to mitigate the oscillation.

Due to the space limitation, only the simulation results of 500MW tie-line power flow are provided in Fig. 8 for comparison. As the system operating point is changed by

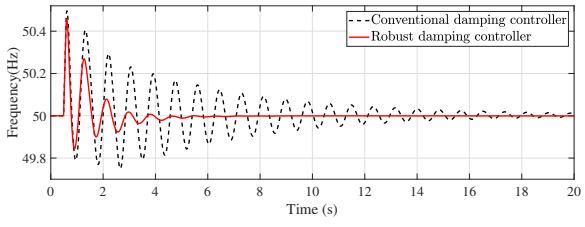


Fig. 7. System frequency response for 400MW tie-line power flow and 15% wind penetration level in a 4M11B system

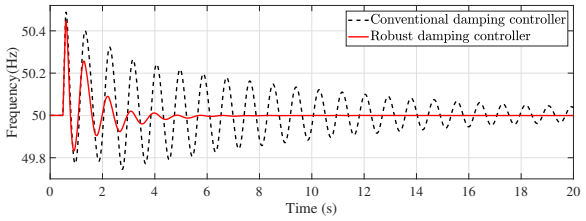


Fig. 8. System frequency response for 500MW power flow in a 4M11B system

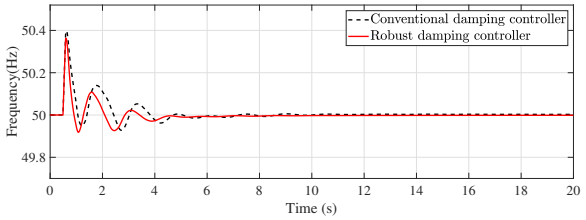


Fig. 9. System frequency response for 30% wind penetration levels in a 4M11B system

increasing the tie-line power flow from 400 MW to 500 MW, it can be seen that the oscillation can still be mitigated within 6 seconds for using a robust damping controller. Based on the simulation results, it can be concluded that the proposed damping controller can provide robust damping performance during tie-line power flow variation. However, for the conventional damping controller, it can be found that the damping performance is different in Fig. 7 and 8 for different tie-line power flows. The simulation results in Fig. 7 and 8 are consistent to the small signal stability results provided in Table IV and V.

Considering the limited space, the simulation results of 15% and 30% wind power penetration levels are selected in this paper for comparing the damping performance of the proposed robust damping controller and conventional damping controller under wind power penetration level variation. Since the nominal operating condition is for 15% DFIG penetration levels in a 4M11B system, the system frequency response is already given in Fig. 7. Fig. 9 shows the system frequency response with 30% DFIG penetration levels. Comparing the results in Fig. 7 and 9, it can be concluded that the robust damping controller can still provide sufficient damping performance and less frequency deviation for different wind power penetration levels. It can also be observed that the damping performance of using a conventional damping controller is varied. The small signal stability analysis results shown in Table VI and VII are verified by system frequency response shown in Fig. 7 and 9.

Throughout the small signal stability analysis results and simulation results provided, it can be found that the damping performance of a conventional damping controller is varied for different system operating conditions. A conventional damping controller cannot provide sufficient damping performance in some operating points. As for the proposed robust damping controller, the damping performance was almost unchanged

under different system operating points. Therefore, it can be concluded that the proposed robust damping controller can mitigate system oscillation caused by FR controller in regardless of uncertain system operating points.

## V. Conclusion

In conclusion, as the grid codes required, widely employed DFIG-based wind turbine are required by system operators to participate system FR when the grid frequency deviation occurs. However, it can be found that a new lightly damped oscillation mode was excited when the DFIG was equipped with FR controller. Considering uncertain system operating points of DFIG-based wind turbine, a robust damping controller was proposed to provide robust damping performance for the new lightly damped oscillation mode. The robust damping controller was designed based on $H_\infty$ control method using LMIs with regional pole placement. In order to verify the robustness of proposed damping controller, a conventional damping controller based on residue method was also modelled. The robust damping performance of the proposed damping controller is verified by installing DFIG with FR controller in a SMIB and 4M11B system using both small signal stability analysis results and simulation results under different system operating points. Results indicated that the proposed damping controller can provide robust damping performance under different system operating points and also less frequency deviation.

## Appendix A
## DFIG parameters

The parameters of the 1.5 MW DFIG are: R=35.25m, $k_{sh} = 1.11$, $D_{sh} = 0.01$, $H_t = 3s$, $H_g = 0.5s$,$L_m = 2.9p.u.$, $L_r = 3.06p.u.$, $L_s = 3.08p.u.$, $L_g = 0.03p.u.$, $R_g = 0.003p.u.$, $K_{p,PLL} = 30$ and $K_{i,PLL} = 1$.

## Appendix B
## 4M11B system parameters

The parameters of generator units G1-G4 under normal operation are: $P_{G1}$ = 900 MW, $Q_{G1}$ = 245 MVAr, $P_{G2}$ = 615 MW, $Q_{G2}$ = 241 MVAr, $P_{G3}$ = 665 MW, $Q_{G3}$ = 76 MVAr, $P_{G4}$ = 665 MW and $Q_{G4}$ = 11 MVAr. For the parameters of loads at buses 8 and 9 are: $P_{L8}$ = 1380 MW, $Q_{L8}$ = 900 MVAr, $P_{L9}$ = 1770 MW and $Q_{GL9}$ = 250 MVAr. Other parameters can be found at [19].

## References


[1] G. P. Prajapat, N. Senroy, and I. N. Kar, "Stability enhancement of dfig-based wind turbine system through linear quadratic regulator," *IET Generation, Transmission Distribution*, vol. 12, no. 6, pp. 1331–1338, Jan 2018.

[2] F. Blaabjerg and K. Ma, "Wind energy systems," *Proceedings of the IEEE*, vol. 105, no. 11, pp. 2116–2131, Nov 2017.

[3] O. G.-B. F. Daz-Gonzlez M. Hau, A.Sumper, "Participation of wind power plants in system frequency control: Review of grid code requirements and control methods," *Renewable and Sustainable Energy Reviews*, vol. 34, pp. 551–564, Jun 2014.

[4] EirGird. (2015) Eirgrid grid code version 6.0. EriGrid, Dublin, Ireland. [Online]. Available: http://www.eirgrid.com

[5] N. G. plc. (2012) The grid code, issue 4 revision 13. National Grid plc, Warwick, U.K. [Online]. Available: http://www.nationalgrid.com/uk/

[6] M. Rahimi, "Dynamic performance assessment of dfig-based wind turbines: A review," *Renewable and Sustainable Energy Reviews*, pp. 852–866, Jun 2014.

[7] J. Morren, S. W. H. de Haan, W. L. Kling, and J. A. Ferreira, "Wind turbines emulating inertia and supporting primary frequency control," *IEEE Transactions on Power Systems*, vol. 21, no. 1, pp. 433–434, Feb 2006.

[8] D. Sun, L. Sun, F. Wu, L. Zhang, W. Geng, J. Peng, and F. Liu, "Research on frequency inertia response control strategy of scess-dfig system considering variable wind speed," *The Journal of Engineering*, vol. 2019, no. 16, pp. 2995–3001, 2019.

[9] H. Geng, X. Xi, L. Liu, G. Yang, and J. Ma, "Hybrid modulated active damping control for dfig-based wind farm participating in frequency response," *IEEE Transactions on Energy Conversion*, vol. 32, no. 3, pp. 1220–1230, Sep. 2017.

[10] Z. Zhang, Y. Sun, J. Lin, and G. Li, "Coordinated frequency regulation by doubly fed induction generator-based wind power plants," *IET Renewable Power Generation*, vol. 6, no. 1, pp. 38–47, January 2012.

[11] Y. Hu and Y. Wu, "Approximation to frequency control capability of a dfig-based wind farm using a simple linear gain droop control," *IEEE Transactions on Industry Applications*, vol. 55, no. 3, pp. 2300–2309, May 2019.

[12] J. Lee, G. Jang, E. Muljadi, F. Blaabjerg, Z. Chen, and Y. Cheol Kang, "Stable short-term frequency support using adaptive gains for a dfig-based wind power plant," *IEEE Transactions on Energy Conversion*, vol. 31, no. 3, pp. 1068–1079, Sep. 2016.

[13] J. Yang, Y. Chen, and Y. Hsu, "Small-signal stability analysis and particle swarm optimisation self-tuning frequency control for an islanding system with dfig wind farm," *IET Generation, Transmission Distribution*, vol. 13, no. 4, pp. 563–574, 2019.

[14] T. K. Chau, S. S. Yu, T. L. Fernando, H. H. Iu, and M. Small, "A novel control strategy of dfig wind turbines in complex power systems for enhancement of primary frequency response and lfod," *IEEE Transactions on Power Systems*, vol. 33, no. 2, pp. 1811–1823, March 2018.

[15] Y. Zhang and A. Bose, "Design of wide-area damping controllers for interarea oscillations," *IEEE Transactions on Power Systems*, vol. 23, no. 3, pp. 1136–1143, Aug 2008.

[16] B. Pal and B. Chaudhuri, *Robust Control in Power Systems*. Springer Science & Business Media, 2005.

[17] M. G. Safonov and R. Y. Chiang, "A schur method for balanced model reduction," *IEEE Transactions on Automat. Control*, vol. 34, no. 7, pp. 729–733, Jul 1989.

[18] N. Yang, Q. Liu, and J. D. McCalley, "Tcsc controller design for damping interarea oscillations," *IEEE Trans. on Power Sys.*, vol. 13, no. 4, pp. 1304–1310, Nov 1998.

[19] P. Kunder, *Power System Stability and Control*. New York: McGraw-Hill, 1994.

[20] H. annele Holttinen and R. Hirvonen, *Wind Power in Power Systems*, T. Ackermann, Ed. West Sussex: John Wiley & Sons, Ltd, 2005.